Journal of Photochemistry and Photobiology A: Chemistry 205 (2009) 179–185

Contents lists available at ScienceDirect

Journal of Photochemistry and Photobiology A: Chemistry

journal homepage: www.elsevier.com/locate/jphotochem

# Important factors for the radiolysis-induced emission intensity of aromatic hydrocarbons

Shingo Samori, Sachiko Tojo, Mamoru Fujitsuka, Tetsuro Majima*

*The Institute of Scientific and Industrial Research (SANKEN), Osaka University, Mihogaoka 8-1, Ibaraki, Osaka 567-0047, Japan*

ARTICLE INFO

*Article history:*
Received 13 February 2008
Received in revised form 10 March 2009
Accepted 4 May 2009
Available online 12 May 2009

*Keywords:*
Aromatic compound
Charge recombination
Fluorescence
Pulse radiolysis
Radical ions

ABSTRACT

Emission from charge recombination between radical cation and anion of various aromatic hydrocarbons (AHs) was observed in the time scales of nanosecond to microsecond during the pulse radiolysis of AH in benzene (Bz). Based on the time-dependent emission study, it is suggested that AH in the excited singlet state ($^1AH^*$) is generated in the nanosecond to microsecond time scale mainly from the charge recombination between AH radical cation ($AH^{\bullet+}$) and AH radical anion ($AH^{\bullet-}$). This mechanism is reasonably explained by the relationship between the annihilation enthalpy change ($-\Delta H^\circ$) for the charge recombination and excitation energies of $^1AH^*$ ($E_{S1}$). It is found that the rate constant of the charge recombination ($k_{rec}$) between $AH^{\bullet+}$ and $AH^{\bullet-}$ increases with the increase of energy differences between $-\Delta H^\circ$ and $E_{S1}$ of AH ($-\Delta H^\circ - E_{S1}$), indicating that the intensity of the radiolysis-induced emission from AH ($I$) depends on ($-\Delta H^\circ - E_{S1}$). The effect of ($-\Delta H^\circ - E_{S1}$) on $I$ value was also examined during the pulse radiolysis of mixtures of two AHs in Bz. Consequently, it is suggested that not only the fluorescence quantum yield ($\Phi_{fl}$) of $^1AH^*$ but also ($-\Delta H^\circ - E_{S1}$) is important factor for the formation yield of $^1AH^*$ during the pulse radiolysis of AH in Bz.



## 1.. Introduction

In the pulse radiolysis of solution, the solvent molecule (S) is initially ionized to give solvent radical cation ($S^{\bullet+}$) and electron ($e^-$) and they form the coulomb-correlated pair ($S^{\bullet+}/e^-$) [1]. Then, S in the excited states ($S^*$) is the main product because $S^*$ should be generated from the geminate recombination of ($S^{\bullet+}/e^-$). In addition, a small fraction of ($S^{\bullet+}/e^-$) is capable of undergoing diffusional escape resulting in the formation of free $S^{\bullet+}$ and $e^-$. These species can react with solute molecule (M) to give M radical cation ($M^{\bullet+}$) and anion ($M^{\bullet-}$), respectively. Thus, it is known that M in the excited state ($M^*$) can be formed from the charge recombination between $M^{\bullet+}$ and $M^{\bullet-}$, as well as energy transfer from $S^*$ to M in a radiolytic process [1–7]. For example, in the pulse radiolysis of M in benzene (Bz), it is known that $M^{\bullet+}$ and $M^{\bullet-}$ can be formed from via positive charge transfer from $Bz^{\bullet+}$ and electron attachment, respectively, and $M^*$ from charge recombination between $M^{\bullet+}$ and $M^{\bullet-}$ as well as energy transfer from $Bz^*$. At low M concentration, the radiation chemical yield of M in the excited singlet state ($^1M^*$) formed by energy transfer from Bz in the excited singlet state ($^1Bz^*$) was negligible because the energy transfer from $^1Bz^*$ to M occurs at diffusion-controlled rate constant ($k_{diff}$). Since the $k_{diff}$ value in Bz is known as $k_{diff} = 1.0 \times 10^{10}\ M^{-1}\ s^{-1}$ [8], the singlet energy transfer from $^1Bz^*$ with the lifetime of 12 ns to M is limited only at M concentration larger than 10 mM [9].

In recent years, we have observed the strong emission from donor–acceptor type molecules with an ethynyl linkage (DEA) such as phenylquinolinylethynes [10], phenyl(9-acridinyl)ethynes [11], phenyl(9-cyanoanthracenyl)ethynes [11,13], and arylethynylpyrenes [12] at the concentration lower than 10 mM during the pulse radiolysis in Bz. Many DEA derivatives have been reported to emit the strong electrogenerated chemiluminescence (ECL), which originates from the charge recombination between $DEA^{\bullet+}$ and $DEA^{\bullet-}$ in solution [14–19]. Using the pulse radiolysis technique, the coinstantaneous formation of $DEA^{\bullet+}$ and $DEA^{\bullet-}$ is assumed for DEA in Bz. In these studies, we proposed that the charge recombination between $DEA^{\bullet+}$ and $DEA^{\bullet-}$ occurred to give DEA in the $S_1$-excited state ($^1DEA^*$) and/or singlet excimer ($^1DEA_2^*$) as the emissive species during the pulse radiolysis. Then, the fluorescence quantum yield ($\Phi_{fl}$), geometry of $DEA^{\bullet+}$ and $DEA^{\bullet-}$, and energy difference between the annihilation enthalpy change ($-\Delta H^\circ$) and the excitation energy ($E_{S1}$) of $^1DEA^*$ ($-\Delta H^\circ - E_{S1}$) were proposed as the factors which governed the intensity of the radiolysis-induced emission from DEA [10–13,20]. However, the suggestions should be reconsidered carefully because our previous reports were carried out for the donor–acceptor type molecules and the suggestions may be limited.

When similar results were observed for the radiolysis-induced emission from various common aromatic hydrocarbons (AHs), it could say that our previously mentioned suggestions have

* Corresponding author. Tel.: +81 6 6879 8495; fax: +81 6 6879 8499.
*E-mail address:* majima@sanken.osaka-u.ac.jp (T. Majima).

1010-6030/$ – see front matter © 2009 Elsevier B.V. All rights reserved.
doi:10.1016/j.jphotochem.2009.05.003

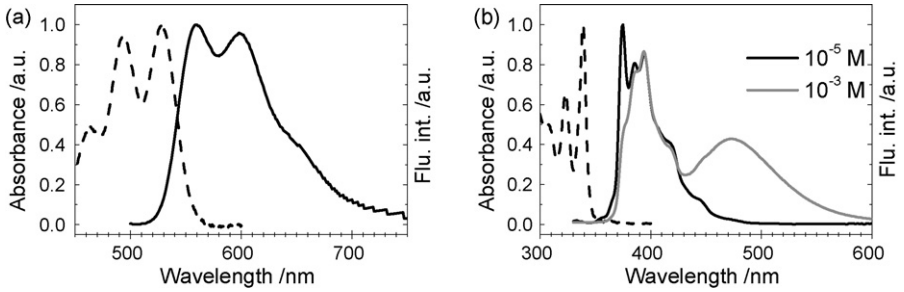


**Fig. 1.** Absorption (broken line) and fluorescence (solid line) spectra observed by the steady-state absorption and fluorescence measurement of Rub (a) ($10^{-5}$ M) and Py (b) ($10^{-5}$ and $10^{-3}$ M) in Ar-saturated Bz. Excitation wavelengths were 430 and 320 nm for Rub and Py, respectively.

the generality. In this paper, therefore, we chose rubrene (Rub), 1,4-bis(phenylethynyl)benzene (bisPEB), 9,10-dimethylanthracene (DMeAn), benzo[k]fluoranthene (B[k]Fl), 9,10-diphenylanthracene (DPhAn), 1-methylpyrene (MePy), pyrene (Py), 2,3-benzofluorene (BF), perylene (Pe), benzo[b]fluoranthene (B[b]Fl), carbazole (Cbz), chrysene (Chry), fluoranthene (Fl), anthracene (An), tetracene (Te), triphenylene (TPh), and thianthrene (Th) as samples. These 17 kinds of AHs show the large changes of $\Phi_{fl}$ values (0.032–0.98) in Bz and oxidation and reduction potentials ($E_{ox}$ = 0.77–2.10 and $E_{red}$ = −2.68 to −1.41 V vs. SCE, respectively) in $CH_3CN$ as described later. In the ECL, the formation of $^1AH^*$ by the charge recombination between $AH^{\bullet+}$ and $AH^{\bullet-}$ has been suggested in many literatures [14–19,21–31]. By measuring the time-resolved transient absorption and emission spectra, the transient species generated during the pulse radiolysis were examined. From the relation between the intensities of the radiolysis-induced emission and the chemical properties of various AHs, the key factors which govern the emission efficiency were shown.

## 2.. Experimental

### 2.1. Materials

Rub, bisPEB, and Chry were purchased from Nacalai Tesque, Wako, and Fluka, respectively. DMeAn, B[k]Fl, DPhAn, Py, B[b]Fl, Fl, Te, and Th were purchased from Aldrich. MePy, BF, Pe, Cbz, An, and TPh were purchased from Tokyo Kasei. All compounds were of the best commercial grade available and used after purification. Bz was purchased from Nacalai Tesque (Spectral grade) and used as a solvent without further purification. All the sample solutions were freshly prepared in 0.1 or 1 mM concentration in Bz in a rectangular quartz cell (1.0 cm × 1.0 cm × 4.0 cm, path length of 1.0 cm). These solutions were saturated with Ar-, air-, or $N_2O$-gas by bubbling for 10 min at room temperature before irradiation. All experiments were carried out at room temperature.

### 2.2. Measurements of steady-state spectral properties

UV spectra were recorded in Bz with a Shimadzu UV-3100PC UV/visible spectrometer. Fluorescence spectra were measured by a Hitachi 850 spectrofluorometer. The fluorescence quantum yields ($\Phi_{fl}$) were determined by using 9,10-diphenylanthracene [32] ($\Phi_{fl}$ = 0.90 in cyclohexane, $\lambda_{ex}$ = 360 nm), and coumarin 334 [33] ($\Phi_{fl}$ = 0.69 in methanol, $\lambda_{ex}$ = 400 nm) standards.

### 2.3. Pulse radiolysis (PR)

Pulse radiolysis experiments were performed using an electron pulse (28 MeV, 8 ns, 0.87 kGy per pulse) from a linear accelerator at Osaka University. The kinetic measurements were performed using

**Table 1**
Steady-state spectroscopic properties of AHs. Absorption maximum ($\lambda^{Abs}_{max}$), fluorescence maximum ($\lambda^{Fl}_{max}$), fluorescence quantum yield ($\Phi_{fl}$), and fluorescence lifetime ($\tau_{fl}$).

| AHs | In Ar-saturated Bz | | | In nonpolar solvent[a] |
|---|---|---|---|---|
| | $\lambda^{Abs}_{max}$ (nm)[b] | $\lambda^{Fl}_{max}$ (nm) | $\Phi_{fl}$ | $\tau_{fl}$ (ns) |
| Rubrene (Rub) | (464), (494), 529 | 560, (598) | 0.98[c] | 16.5[c] |
| 1,4-Bis(phenylethynyl)benzene (bisPEB) | 322 | 350, (364) | 0.90 | 0.63[d] |
| 9,10-Dimethylanthracene (DMeAn) | (359), 381, (402) | (409), 432, (458) | 0.90 | 14.0[c] |
| Benzo[k]fluoranthene (B[k]Fl) | (362), (381), 404 | (409), 434, (461) | 0.85 | 11.3[c] |
| 9,10-Diphenylanthracene (DPhAn) | (357), 375, (396) | (411), 430 | 0.84 | 7.7[c] |
| 1-Methylpyrene (MePy) | (330), 347 | 378, (398), (419) | 0.81 | 255[e] |
| Pyrene (Py) | (323), 339 | 375, (386), (394) | 0.74 | 650[c] |
| 2,3-Benzofluorene (BF) | 306, (320), (342) | 343, (360) | 0.63 | nd |
| Perylene (Pe) | (391), (412), 439 | 445, (473), (505) | 0.53 | 6.4[c] |
| Benzo[b]fluoranthene (B[b]Fl) | 352, (370) | 456 | 0.44 | 44.3[c] |
| Carbazole (Cbz) | 336 | 341, (355) | 0.32 | 16.1[c] |
| Chrysene (Chry) | 309, (323) | 364, (383), (405), (429) | 0.27 | 44.7[c] |
| Fluoranthene (Fl) | (310), (325), (345), 361 | 467 | 0.22 | 53[c] |
| Anthracene (An) | (326), (342), 359, (379) | (384), 405, (428), (454) | 0.19 | 5.3[c] |
| Tetracene (Te) | (397), (419), (445), 475 | 479, (513), (550), (592) | 0.15 | 6.4[c] |
| Triphenylene (TPh) | 288 | 356 | 0.072 | 36.6[c] |
| Thianthrene (Th) | <340[f] | 450 | 0.032 | 29[g] |

[a] Such as cyclohexane, *n*-heptane, and isooctane, etc.
[b] The values in parenthesis are the maxima of vibronic peaks.
[c] Ref. [35].
[d] Ref. [36].
[e] Ref. [37].
[f] No peak at wavelength longer than 340 nm.
[g] Ref. [38].

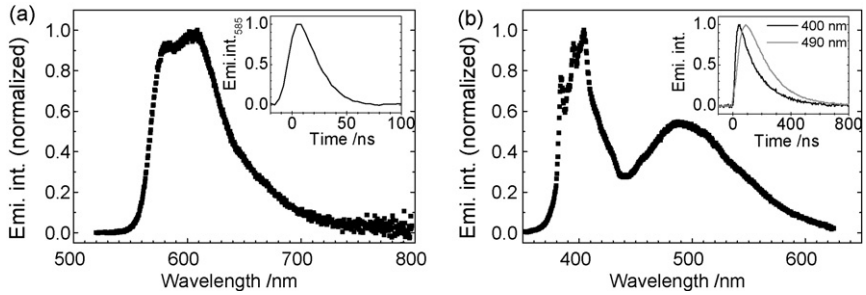


**Fig. 2.** Radiolysis-induced emission spectra observed immediately after an electron pulse during the pulse radiolysis of Rub (a) and Py (b) in Ar-saturated Bz (1 mM). *Insets*: time profiles of the emission observed at the emission peaks.

**Table 2**
Emission maxima ($\lambda_{max}^{Em}$) and relative emission intensity ($I$) of the radiolysis-induced emission spectra of AHs in Ar-, Air-, and $N_2O$-saturated Bz (1 mM), and emission half lifetime ($\tau_{1/2}$) in Ar-saturated Bz.

| AHs | $\lambda_{max}^{Em}$ (nm) | $I$[a] (%) | | | $\tau_{1/2}$ (ns) |
|---|---|---|---|---|---|
| | | Ar | Air | $N_2O$ | Ar |
| Rub[b] | 609 | 106 | 46.7 | 24.9 | 15 |
| bisPEB[b] | 376 | 233 | 92.2 | 140 | < 8 |
| DMeAn[b] | 439, (426), (466) | 148 | 54.5 | 90.6 | 14 |
| B[k]Fl[b] | 440, (467) | 187 | 78.0 | 119 | 18 |
| DPhAn[b] | 440 | 181 | 77.9 | 118 | <8 |
| MePy | 407, (388), $(486)_{ex}$ | 117 | 66.6 | 81.3 | 25–58 |
| Py | 404, (384), (395) | 129 | 59.4 | 109 | 104–138 |
| BF[b] | 368, (360) | 267 | 62.7 | 182 | 28 |
| Pe[b] | 483, (517) | 130 | 59.4 | 70.3 | <8 |
| B[b]Fl | 443, (461) | 100 | 62.7 | 63.8 | 36 |
| Cbz[b] | 365 | 163 | 54.1 | 121 | 15 |
| Chry[b] | 392, (374), (413), (436) | 81.3 | 15.1 | 53.3 | 38 |
| Fl | 476 | 82.8 | 29.8 | 38.5 | 40 |
| An | 413, (399), (434), (463) | 38.8 | 16.3 | 29.4 | 13 |
| Te[b] (sat.)[c] | 523, (497), (561) | 11.4 | 5.48 | 7.15 | <8 |
| TPh | 364, (372), (381) | 40.9 | 8.36 | 25.5 | 34 |
| Th | 442 | 12.9 | 4.55 | 8.83 | 20 |

[a] Relative to $I$ value of B[b]Fl in Ar-saturated Bz.
[b] $I$ value was reduced due to the self-absorption as a result of high concentration of AHs.
[c] Saturated concentration due to poor solubility.

a nanosecond photoreaction analyzer system (Unisoku, TSP-1000). The monitor light was obtained from a pulsed 450-W Xe arc lamp (Ushio, UXL-451-0), which was operated by a large current pulsed-power supply that was synchronized with the electron pulse. The monitor light was passed through an iris with a diameter of 0.2 cm and sent into the sample solution at a perpendicular intersection to the electron pulse. The monitor light passing through the sample was focused on the entrance slit of a monochromator (Unisoku, MD200) and detected with a photomultiplier tube (Hamamatsu Photonics, R2949). The transient absorption and emission spectra

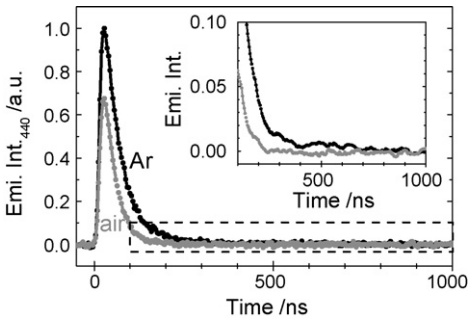


**Fig. 3.** Time profiles of emission at 440 nm observed during the pulse radiolysis of B[b]Fl with Ar- and air-saturated Bz. *Inset*: time profiles in the 100–1000 ns region indicated by the broken line.

were measured using a photodiode array (Hamamatsu Photonics, S3904-1024F) with a gated image intensifier (Hamamatsu Photonics, C2925-01) as a detector. All emission spectra were corrected for the spectral sensitivity of the apparatus. The emission intensities ($I$) of all AHs were estimated based on the integration values of emission spectra observed in the time scales of nanosecond to microsecond during pulse radiolysis. In order to clarify the intermediate species formed in this system, which would alter the emission intensity ($I$), $N_2O$ and $O_2$, as a quencher of the intermediate species, at the concentration of the millimolar order were added to solution. To avoid pyrolysis of the sample solution by the monitor light, a suitable cutoff filter was used.

### 2.4. Measurements of electrochemical properties

Oxidation ($E_{ox}$) and reduction potentials ($E_{red}$) were measured by cyclic voltammetry (BAS, CV-50W) with platinum working and auxiliary electrodes and an $Ag/Ag^+$ reference electrode at a scan rate of 100 mV $s^{-1}$. Measurements were performed in dry acetonitrile containing approximately 1 mM of AHs and 0.1 M tetraethylammonium perchlorate.

## 3.. Results and discussion

### 3.1. Steady-state spectral properties of AHs

At first, the steady-state absorption and fluorescence spectra of AHs were measured in order to examine their $S_1$-excited state properties. Fig. 1(a) and (b) shows the steady-state absorption and fluorescence spectra of Rub and Py, respectively. At 1 mM concentration, the fluorescence spectra of both Py and MePy showed monomer and excimer emission maxima although all other AHs showed only monomer emission maxima. It is well known that the large $\pi$ surface of pyrene is favorable to interact with each other. At the high pyrene concentration, therefore, $\pi$-stacking interaction between two pyrene units in the excited state results in the excimer emission upon photoexcitation. The steady-state absorption and fluorescence spectral data of AHs are summarized in Table 1.

### 3.2. Emission generated from charge recombination between $AH^{\bullet+}$ and $AH^{\bullet-}$

Next, the emission spectra were measured using the pulse radiolysis technique. Emission spectra appeared within an electron pulse of 8 ns during the pulse radiolysis of all AHs (1 mM) in Ar-saturated Bz. Fig. 2(a) and (b) shows the emission spectra observed during the pulse radiolysis of Rub and Py in Ar-saturated Bz (1 mM). The shape of the radiolysis-induced emission spectra of Rub was different from that observed in the steady-state measurement and emission maxima observed at shorter wavelength region disappeared because of the strong self-absorption as a result

of the high concentrations (1 mM) [10–13,20]. The self-absorption was observed for not only Rub but also many other AHs. The radiolysis-induced emission spectra of Py and MePy also showed both monomer and excimer emissions, although other AHs showed no excimer emission.

The emission intensities ($I$) of AHs (1 mM) were determined from the total amount of the radiolysis-induced emission as summarized in Table 2. When air (in the presence of dissolved oxygen) was added to the solution as the electron scavenger and triplet quencher, $I$ values of AHs were reduced. When $N_2O$ gas was added to the solution as the electron (radical anion) scavenger, $I$ were also reduced by 23–84%. These results suggest that electron and/or $AH^{\bullet-}$ is responsible for the emission during the pulse radiolysis. The difference of $I$ values in the presence of $N_2O$ and air is due to the differences of the intermediate species quenched and the concentrations of $N_2O$ and air (saturated concentration in Bz: 400 mM [34] and 1.9 mM [35], respectively).

It should be noted that $I$ values of bisPEB (233) and BF (267) are higher than that of Rub (106), although $\Phi_{fl}$ values of bisPEB (0.90) and BF (0.63) are lower than that of Rub (0.98) in Ar-saturated Bz. The radiolysis-induced emission spectra of these three AHs showed the self-absorption due to high concentration. $I$ values of these AHs were corrected based on the fluorescence spectra obtained by the steady-state measurement.

The emission time profiles observed during the pulse radiolysis of AHs in Ar-saturated Bz showed two components having short-lifetime with high emission intensity and long-lifetime with very low intensity. As an example, the time profile of the radiolysis-induced emission was shown in Fig. 3 for B[b]Fl in Ar- and air-saturated Bz observed at 440 nm during the pulse radiolysis. In Ar-saturated Bz, the emission time profile clearly showed two components: short-lived and long-lived components with lifetimes of several tens and hundreds nanoseconds, respectively. In air saturated Bz (in the presence of dissolved oxygen), the emission time profile showed no long-lived emission component.

The half lifetimes ($\tau_{1/2}$) of the short-lived emission from AHs in Bz were found to be almost similar to the reported fluorescence lifetimes ($\tau_{fl}$) of AHs in nonpolar solvents, except for Py and MePy which showed the excimer emission with larger lifetimes (Table 1). As a result, the formation of the emissive species $^1AH^*$ (for all AHs) and $^1AH_2{}^*$ (for Py and MePy) can be assumed at the several tens nanoseconds after an electron pulse. Even at a few μs after an electron pulse, the long-lived emission was observed for all AHs. There was no difference in the emission spectra observed immediately (at a few tens nanosecond) and at a few microsecond after an electron pulse. Since this long-lived emission was quenched by oxygen, it can be assigned to the "P-type" delayed fluorescence [39,40] resulted from the triplet–triplet annihilation of $^3AH^*$ [10–13,20]. The lifetimes of the long-lived emission observed for all AHs were almost equivalent with those of $^3AHs^*$, indicating the long-lived emission to be the "P-type" delayed fluorescence.

Fig. 4 shows the plots of $I$ values vs. $\Phi_{fl}$ values for AHs in Bz. Since the emission intensities of some AHs are lower than their true values due to the self-absorption, $I$ values of some AHs are corrected as shown in Fig. 4, open squares. This figure clearly showed that $I$ values showed little dependence on $\Phi_{fl}$ values. Thus, it is suggested that not only $\Phi_{fl}$ but also other factor govern $I$ value of AHs.

To elucidate the emission mechanism of AHs, the electrochemical properties (oxidation and reduction potentials) were measured by cyclic voltammetry. It has been well known that the annihilation enthalpy change ($-\Delta H^\circ$) value for the charge recombination between $AH^{\bullet+}$ and $AH^{\bullet-}$ is criterion whether $^1AH^*$ can be energetically formed from the charge recombination or not [14–19,21–23]. This $-\Delta H^\circ$ value is calculated from Eqs. (1)–(3) [41],

$$-\Delta H^\circ = [(E_{ox} - E_{red})]\varepsilon_s - \Delta G_{sol}\varepsilon_s - w_{a,\mu} + T\Delta S^\circ \quad (1)$$

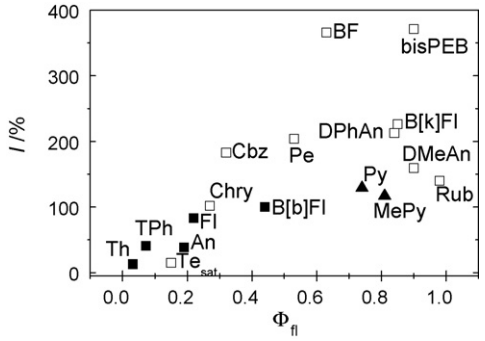


**Fig. 4.** Plots of $I$ value (%) vs. $\Phi_{fl}$ for AHs in Bz. Since $I$ values of some AHs are lower than those true values due to the self-absorption, some $I$ values are corrected based on the fluorescence spectra obtained by the steady-state measurement (open squares). For Py and MePy, both monomer and excimer emissions were observed (solid triangle).

$$\Delta G_{sol}\varepsilon_s = -\left(\frac{e^2}{2}\right)\left(\frac{1}{r_D} + \frac{1}{r_A}\right)\left(1 - \frac{1}{\varepsilon_s}\right) \quad (2)$$

$$w_{a,\mu} = -\frac{e^2}{\varepsilon_s d_{cc}}, \quad (3)$$

where $E_{ox}$ and $E_{red}$ are the oxidation and reduction potentials of AH, respectively. $\varepsilon_s$, $\Delta G_{sol}$, and $w_{a,\mu}$ represent the static dielectric constant of solvent (Bz: $\varepsilon_s = 2.284$) [35], the free energy change of solvation, and the work required to bring $AH^{\bullet+}$ and $AH^{\bullet-}$ within a likely separation distance, respectively. $e$, $r_D$, $r_A$, and $d_{cc}$ represent elementary charge, radii $AH^{\bullet+}$ and $AH^{\bullet-}$, and reaction distance between $AH^{\bullet+}$ and $AH^{\bullet-}$, respectively. The radii $r_D$ and $r_A$ were roughly determined from $r = (3M/4\pi\rho N_A)^{1/3}$, where $M$, $\rho$, and $N_A$ were molecular weight, molecular density of AHs, and the Avogadro number, respectively. The $d_{cc}$ was considered to be equal to the sum of the average $r_D$ and $r_A$ values [42]. The precise value for $T\Delta S^\circ$ is unknown, but it was estimated to be $\sim 0.1 \pm 0.1$ eV [21–23]. As a result, the estimated $-\Delta H^\circ$ are listed in Table 3. The excitation energy of $^1AH^*$ ($E_{S1}$) was determined from the wavelength at the intersection point between the absorption spectrum and radiolysis-induced emission spectrum normalized in view of the self-absorption (Table 3). The $-\Delta H^\circ$ values for all AHs (2.61–5.13 eV) are consistently larger than their $E_{S1}$ values (2.23–3.76 eV), indicating that the energy available in the charge recombination is sufficient to generate $^1AH^*$ for all AHs.

The transient absorption spectra of AHs were also measured during the pulse radiolysis of AHs in Ar-saturated Bz. All AHs showed the characteristic transient absorption spectra. According to literatures [32], these transient absorption spectra are assigned mainly to $^3AH^*$ for all AHs. In the pulse radiolysis of M in Bz, the energy transfer from $^3Bz^*$ to AH occurs to give $^3AH^*$ ($^3Bz^* + AH \rightarrow Bz + {}^3AH^*$) [9]. No transient absorption band of $AH^{\bullet+}$ and $AH^{\bullet-}$ was observed immediately after an 8-ns electron pulse in Bz, indicating that $^1AH^*$ was formed from the charge recombination between $AH^{\bullet+}$ and $AH^{\bullet-}$ within a pulse duration of 8 ns [10–13,20].

### 3.3. Emission mechanism

A plausible mechanism of the emission during the pulse radiolysis of AHs in Bz is shown in Scheme 1. The charge recombination between $AH^{\bullet+}$ and $AH^{\bullet-}$ occurs to give $^1AH^*$, $^3AH^*$, AH in the ground state and $^1(AH)_2{}^*$ (for Py and MePy) during the pulse radiolysis of AHs in Bz. In addition, the delayed fluorescence (long-lived emission component with very low intensity) also occurs through the triplet–triplet annihilation of $^3AH^*$.

As indicated in Fig. 4, $I$ values of AHs showed a little dependence on $\Phi_{fl}$. However, $I$ values of bisPEB and BF with relatively

**Table 3**
Annihilation enthalpy changes ($-\Delta H^\circ$) and ($-\Delta H^\circ - E_{S1}$) of AHs calculated from $E_{S1}$, oxidation ($E_{ox}$), and reduction potentials ($E_{red}$).

| AHs | $E_{S1}$[a] (eV) in Bz | $E_{T1}$[b] (eV) | In $CH_3CN$ | | In Bz | |
|---|---|---|---|---|---|---|
| | | | $E_{ox}$ (V vs. SCE) | $E_{red}$ (V vs. SCE) | $-\Delta H^\circ$ (eV) | $-\Delta H^\circ - E_{S1}$ (eV) |
| Rub | 2.23 | 1.04[c] | 0.82[c] | −1.41[c] | 2.61 | + 0.38 |
| bisPEB | 3.52 | – | 1.67[d] | −2.10[d] | 4.27 | +0.75 |
| DMeAn | 3.01 | 1.80[c] | 0.87[c] | −1.82[c] | 3.24 | +0.23 |
| B[k]Fl | 3.00 | 2.19[e] | 1.24[e] | −1.79 | 3.57 | +0.57 |
| DPhAn | 3.02 | 1.81[c] | 1.20[c] | −1.84[c] | 3.51 | +0.49 |
| MePy | 3.37 | – | 1.53[f] | −2.15[g] | 4.25 | +0.88 |
| Py | 3.42 | 2.08[c] | 1.36[c] | −2.09[c] | 4.04 | +0.62 |
| BF | 3.59 | 2.49[h] | 2.10[i] | −2.47 | 5.13 | +1.54 |
| Pe | 2.73 | 1.56[c] | 0.85[c] | −1.67[c] | 3.06 | +0.33 |
| B[b]Fl | 3.18 | 2.37[e] | 1.41[e] | −1.77 | 3.72 | +0.54 |
| Cbz | 3.60 | 3.04[c] | 1.16[c] | −2.68[c] | 4.47 | +0.87 |
| Chry | 3.60 | 2.48[d] | 1.35[j] | −2.30[j] | 4.19 | +0.59 |
| Fl | 3.10 | 2.29[c] | 1.48[c] | −1.74[c] | 3.76 | +0.66 |
| An | 3.20 | 1.82[c] | 1.20[c] | −1.92[c] | 3.71 | +0.51 |
| Te | 2.55 | 1.28[d] | 0.77[j] | −1.55[j] | 2.87 | +0.32 |
| TPh | 3.76 | 2.89[d] | 1.55[j] | −2.41[j] | 4.51 | +0.75 |
| Th | 3.26 | 2.60[c] | 1.22[c] | −2.54[c] | 4.34 | +1.08 |

[a] $E_{S1}$ values were determined from the wavelength at the intersection point between the absorption spectrum and radiolysis-induced emission spectrum normalized with respect of the self-absorption.
[b] $T_1$-state excitation energies ($E_{T1}$) of AHs in various solvents such as Bz and $CH_3CN$, etc.
[c] Ref. [43].
[d] Ref. [44].
[e] Ref. [45].
[f] Ref. [46].
[g] Ref. [47].
[h] Ref. [35].
[i] Ref. [48].
[j] Ref. [49].

higher $-\Delta H^\circ$ value were very high and away from the relation. This result implies that not only $\Phi_{fl}$ but also other factor which relates to $-\Delta H^\circ$ governs $I$ values of AHs. In our previous paper [20], the energy differences between $-\Delta H^\circ$ and $E_{S1}$ ($-\Delta H^\circ - E_{S1}$) was assumed as the one of the key factor for $I$ value. Thus, the ($-\Delta H^\circ - E_{S1}$) values of AHs are estimated and listed in Table 3. The formation of $^1AH^*$ by the charge recombination between $AH^{\bullet+}$ and $AH^{\bullet-}$ occurs when $-\Delta H^\circ$ is sufficiently larger than $E_{S1}$ value. In other words, the energy amount required to attain $^1AH^*$ is equivalent to $E_{S1}$ value, and then ($-\Delta H^\circ - E_{S1}$) value means only excess energy. In the following section, we discussed the effect of ($-\Delta H^\circ - E_{S1}$) value on the radiolysis-induced emission of AHs.

$$Bz \rightsquigarrow e^- + Bz^{\bullet+} \quad (4)$$

$$Bz^{\bullet+} + e^- \rightarrow Bz^* \quad (5)$$

$$Bz^{\bullet+} + AH \rightarrow AH^{\bullet+} \quad (6)$$

$$e^- + AH \rightarrow AH^{\bullet-} \quad (7)$$

$$^3Bz^* + AH \rightarrow Bz + {}^3AH^* \quad (8)$$

$$AH^{\bullet+} + AH^{\bullet-} \xrightarrow{k_S} {}^1AH^* + AH \quad (9)$$

$$AH^{\bullet+} + AH^{\bullet-} \xrightarrow{k_T} {}^3AH^* + AH \quad (10)$$

$$AH^{\bullet+} + AH^{\bullet-} \xrightarrow{k_{gs}} 2AH \quad (11)$$

$$AH^{\bullet+} + AH^{\bullet-} \rightarrow {}^1AH^* + AH,\ {}^3AH^* + AH, \text{ and } {}^1(AH)_2^* \text{ (for Py and MePy)} \quad (12)$$

$$e^- + AH^{\bullet+} \rightarrow AH^* \quad (13)$$

$$Bz^{\bullet+} + AH^{\bullet-} \rightarrow Bz + AH^* \quad (14)$$

$$^3AH^* + {}^3AH^* \rightarrow {}^1AH^* + AH \quad (15)$$

$$^3AH^* + {}^3AH^* \rightarrow {}^1AH^* + AH \text{ and } {}^1(AH)_2^* \text{ (for Py and MePy)} \quad (16)$$

$$^1AH^* \rightarrow AH + h\nu_{fl} \text{ (ps - ns)} \quad (17)$$

$$^1AH^* \rightarrow AH + h\nu_{df} \text{ (ns - μs)} \quad (18)$$

$$^1(AH)_2^* \rightarrow 2AH + h\nu_{ex} \text{ (for Py and MePy)} \quad (19)$$

**Scheme 1.** Plausible mechanism of the emission during pulse radiolysis of AHs in Bz. $k_S$, $k_T$ and $k_{gs}$ denote the rate constants for the charge recombination to give $^1AH^*$, $^3AH^*$ and AH in the ground state, respectively. $h\nu_{fl}$, $h\nu_{ex}$, and $h\nu_{df}$ denote fluorescence from monomer, excimer, and P-type delayed emission derived from triplet–triplet annihilation, respectively.

### 3.4. The effect of ($-\Delta H^\circ - E_{S1}$) value on the radiolysis-induced emission of AHs

The Gibbs free energy ($\Delta G$) for the reaction of $AH^{\bullet+}$ and $AH^{\bullet-}$ can be expressed by Eq. (20) [50],

$$\Delta G = \Delta G_{gs} + \Delta G_{es} + w_{a,\mu}, \quad (20)$$

where $\Delta G_{gs}$ is the free energy change associated with direct formation of the ground state as determined from $\Delta E = E^\circ_{red} - E^\circ_{ox}$, and $\Delta G_{es}$ is the energy required to reach $^1AH^*$ or $^3AH^*$ ($E_{S1}$ or $E_{T1}$, respectively). Using $\Delta H^\circ$ and $\Delta G_{es}$, $\Delta G$ can be expressed by Eq. (21) [41],

$$\Delta G = \Delta H^\circ + T\Delta S^\circ + \Delta G_{es}. \quad (21)$$

Since $T\Delta S^\circ$ value for this kind of reaction is negligible small (typically only about 0.1 eV), ($-\Delta H^\circ - E_{S1}$) can be estimated to be approximately equivalent to $-\Delta G$ for the charge recombination between $AH^{\bullet+}$ and $AH^{\bullet-}$ to produce $^1AH^*$ [21–23].

The charge recombination between $AH^{\bullet+}$ and $AH^{\bullet-}$ to give $AH^*$ ($^1AH^*$ and $^3AH^*$) can be considered as the electron transfer reaction in which $AH^*$ is formed as a consequence of formation of an encounter complex of the radical ions ($AH^{\bullet+}/AH^{\bullet-}$) as shown in Eq. (22) [13]:

$$AH^{\bullet+} + AH^{\bullet-} \underset{k_{-d}}{\overset{k_d}{\rightleftarrows}} AH^{\bullet+}/AH^{\bullet-} \xrightarrow{k_{rec}} AH^* + AH, \quad (22)$$

where $k_d$, $k_{-d}$ and $k_{rec}$ are the diffusion-controlled rate constants for the formation of the encounter complex, dissociation of $AH^{\bullet+}/AH^{\bullet-}$ into free $AH^{\bullet+}$ and $AH^{\bullet-}$, and the charge recombination to give $AH^*$, respectively. Thus, the apparent rate constant for the charge recombination between $AH^{\bullet+}$ and $AH^{\bullet-}$ to give $AH^*$ ($k'_{rec}$) is represented by these rate constants,

$$k'_{rec} = \frac{k_{rec}k_d}{k_{rec} + k_{-d}}. \quad (23)$$

In ECL study, ECL efficiency ($\eta_{ECL}$) was expressed by $\Phi_{fl}$ and some bimolecular electron transfer rates [50–52]. Similarly, $I$ value of AH can be expressed as,

$$I \approx \frac{A\Phi_{fl}k_S}{k_S + 3k_T + k_{gs}} \quad (24)$$

where $A$ is a correction factor, and $k_S$, $k_T$ and $k_{gs}$ are the electron-transfer rate constant for the charge recombination between $AH^{\bullet+}$ and $AH^{\bullet-}$ to give $^1AH^*$, $^3AH^*$ and AH in the ground state, respectively. These rates should be expressed by a statistical factor determined by the spin distribution [53]. Since the delayed fluorescence resulted from the triplet–triplet annihilation of $^3AH^*$ was too weak, this process was not included in Eq. (8).

According to the classical Marcus electron transfer theory [8], $k_{rec}$ is related to $\Delta G$ as shown in Eq. (25),

$$k_{rec} \propto \exp\left[\frac{-(\Delta G - \lambda)^2}{4\lambda k_B T}\right] \quad (25)$$

where $k_B$ is Boltzmann's constant, $T$ is temperature, and $\lambda$ is the sum of the inner-sphere ($\lambda_V$) and the outer-sphere reorganization energies ($\lambda_S$). Thus, as $\Delta G$ becomes more negative, $k_{rec}$ increases until the magnitude of $\Delta G$ becomes equal to $\lambda$, then decreases as $\Delta G$ becomes larger in magnitude than $\lambda$. By Eq. (25), it is reasonably explained that the increase of $(-\Delta H^\circ - E_{S1})$ ($\approx -\Delta G$) leads to the increase of $k_{rec}$.

The $\lambda_S$ value for this system is assumed to be negligible due to the low relative permittivity ($\varepsilon_S$) of Bz. While $\lambda_V$ value has reported to be 0.6 eV for similar aromatic compounds [54]. Thus, $\lambda$ value can be estimated to be ~0.6 eV for the charge recombination between $AH^{\bullet+}$ and $AH^{\bullet-}$ in Bz. Then, the $-\Delta G$ for the charge recombination between $AH^{\bullet+}$ and $AH^{\bullet-}$ to produce $^1AH^*$ ($-\Delta G = -\Delta H^\circ - E_{S1}$) is assumed to mainly locate in the Marcus normal region ($-\Delta G < \lambda$) and that to produce AH in the ground state ($-\Delta G = -\Delta H^\circ$) far into the inverted region ($\lambda < -\Delta G$) [55]. Thus, the increase of $-\Delta G$ will increase $k_S$ value, while $k_{gs}$ is decreased. The $-\Delta G$ for the charge recombination between $AH^{\bullet+}$ and $AH^{\bullet-}$ to produce $^3AH^*$ ($-\Delta G = -\Delta H^\circ - E_{T1}$) is estimated to be slightly larger than that to produce $^1AH^*$. Similar calculations show that $k_T$ is near its maximum, which exceeds $k_{-d}$ [50]. Thus, from Eq. (23) $k_T$ becomes equal to $k_d$. As such, it should be little affected by changes in $-\Delta G$. Substitution of Eq. (23) for the formation of $^1AH^*$ with $k_T = k_d$ reduces Eq. (24) to

$$I \approx \frac{A\Phi_{fl}k_{rec}}{4k_{rec} + 3k_{-d}} \quad (26)$$

with the assumption that $k_{gs}$ is sufficiently inverted as to be insignificant. Thus, an increase in $k_{rec}$ resulting from a change in $-\Delta G$ will result in an increase in $I$ value.

Fig. 5 shows the plots of $\ln(I/\Phi_{fl})$ vs. $(-\Delta H^\circ - E_{S1})$ for AHs. In order to evaluate not the emission efficiency from $^1AH^*$ but the formation efficiency of $^1AH^*$, $I$ value was divided by $\Phi_{fl}$ value and plotted vs. $(-\Delta H^\circ - E_{S1})$. Except for Py and MePy, the emission efficiency increases as $(-\Delta H^\circ - E_{S1})$ becomes larger. The deviations for the plots of Py and MePy were explained by the formation of excimers with low emission intensities. The plot of BF with high $(-\Delta H^\circ - E_{S1})$ value seems to reach a plateau. Similar result was obtained for previous report on

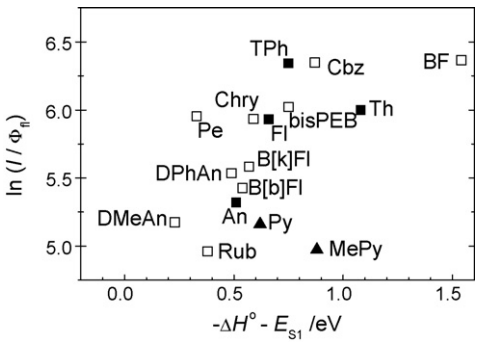


**Fig. 5.** Plots of the $\ln(I/\Phi_{fl})$ vs. $(-\Delta H^\circ - E_{S1})$ for AHs in Bz.

allied donor–acceptor type compounds. The plots of $\ln(I/\Phi_{fl})$ vs. $(-\Delta H^\circ - E_{S1})$ for 9-cyano-10-(*p*-substituted phenyl)anthracene (RAN) [20] in Bz also shows the increase of the emission efficiency with the increase of $(-\Delta H^\circ - E_{S1})$ (Fig. S1, Supplementary data). Similar plot which showed ECL efficiency increased with an increase in $-\Delta G$, and then reached a plateau, has reported for ECL from aluminum quinolates and quinacridones occurred by the cross reaction with triarylamines in mixed solvent including Bz [39,40]. As a result, it can be explained that $(-\Delta H^\circ - E_{S1})$ value alters $I$ values of AHs. Consequently, it is found that the exothermic energy generated from the charge recombination between $AH^{\bullet+}$ and $AH^{\bullet-}$ is important factor for the formation yield of $^1AH^*$.

### 3.5. Emission spectrum during the pulse radiolysis of mixture of AHs

Finally, we measured the emission spectrum during the pulse radiolysis of mixture of AHs in Ar-saturated Bz. We used the mixture of An and Fl as the sample because their $\Phi_{fl}$ values are almost the same (0.19 and 0.22, respectively) and An and Fl can prevent the problem of self-absorption due to their large Stokes shifts. Fig. 6(a) shows the emission spectrum observed during the pulse radiolysis of a mixture of An (0.1 mM) and Fl (0.1 mM) in Ar-saturated Bz. While Fig. 6(b) shows the fluorescence spectrum observed by the steady-state fluorescence measurement of the mixture of An (0.1 mM) and Fl (0.1 mM) in Ar-saturated Bz. In the steady-state fluorescence measurement, the sample solution was excited at 372 nm since An (0.1 mM) and Fl (0.1 mM) have the same absorbance at 372 nm. These fluorescence spectra were divided to the An and Fl fluorescence components (Fig. 6, dashed lines). The ratio of the Fl to An fluorescence component was 1.94 in the radiolysis-induced emission spectrum, while that was 1.55 in the steady-state fluorescence spectrum. In other words, the formation ratio of $^1Fl^*$ during the pulse radiolysis of the mixture of An and Fl was larger than that obtained by the steady-state fluorescence measurement. The estimated $-\Delta H^\circ$ values for the charge recombination between $An^{\bullet+}$ and $Fl^{\bullet-}$ is 3.51 eV, and that for $An^{\bullet-}$ and $Fl^{\bullet+}$ is 3.97 eV. Since $E_{S1}$ values of An and Fl are 3.20 and 3.10 eV, respectively, $-\Delta H^\circ$ values for these systems are sufficiently larger than their $E_{S1}$ values, indicating that the energy available in the charge recombination is sufficient to generate both An and Fl in the $S_1$ state. As described above, $I$ value depends on the $(-\Delta H^\circ - E_{S1})$. Thus, the larger $(-\Delta H^\circ - E_{S1})$ values for the formation of $^1Fl^*$ (0.87–0.41 eV) than that of $^1An^*$ (0.77–0.31 eV) are assumed to alter the formation ratio of $^1Fl^*$ during the pulse radiolysis. Consequently, it is clarified that $(-\Delta H^\circ - E_{S1})$ values are also important factor for $I$ value observed during the pulse radiolysis of a mixture of several AHs in Ar-saturated Bz.

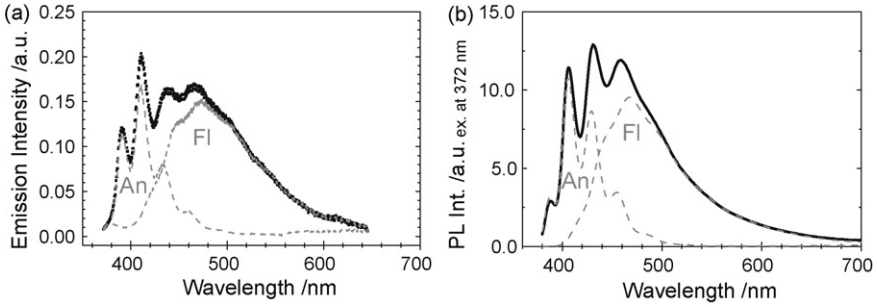


**Fig. 6.** Emission spectrum observed during the pulse radiolysis (a) and fluorescence spectrum observed by the steady-state fluorescence measurement (b) of mixture of An (0.1 mM) and Fl (0.1 mM) in Ar-saturated Bz. These spectra are divided to two (An and Fl) components (dashed lines).

## 4.. Conclusion

Various AHs showed the emission in the time scales of nanosecond to microsecond during the pulse radiolysis of AH in Bz. The emission is suggested to be originated from $^1AH^*$ generated mainly by the charge recombination between $AH^{\bullet+}$ and $AH^{\bullet-}$ which are yielded from the initial radiolytic reaction in Bz. This mechanism is reasonably explained by the fact that relationship between $-\Delta H^\circ$ values (2.61–5.13 eV) estimated for the charge recombination between $AH^{\bullet+}$ and $AH^{\bullet-}$ are sufficiently larger than the $S_1$-state excitation energies ($E_{S1}$) of AHs (2.23–3.76 eV). From the relation between $\ln(I/\Phi_{fl})$ vs. $(-\Delta H^\circ - E_{S1})$, it was clearly shown that not only the $\Phi_{fl}$ of AH but also the energy differences between $-\Delta H^\circ$ and $E_{S1}$ of AH $(-\Delta H^\circ - E_{S1})$, which corresponds to the exothermic energy during the charge recombination, are important factors for $I$ values of AHs.

## Supplementary data

Supplementary data available: Plots of the $\ln(I/\Phi_{fl})$ vs. $(-\Delta H^\circ - E_{S1})$ for 9-cyano-10-(p-substituted phenyl)anthracene (RAN) in Bz (Fig. S1).

## Acknowledgments

We thank the members of the Radiation Laboratory of ISIR, Osaka Univ. for running the linear accelerator. This work has been partly supported by a Grant-in-Aid for Scientific Research (Project 17105005, 19350069, and others) from the Ministry of Education, Culture, Sports, Science and Technology (MEXT) of Japanese Government. One of the authors (S.S.) expresses his thanks for JSPS Research Fellowship for Young Scientists and the Global COE Program "Global Education and Research Center for Bio-Environmental Chemistry" of Osaka University.

## Appendix A. Supplementary data

Supplementary data associated with this article can be found, in the online version, at doi:10.1016/j.jphotochem.2009.05.003.

## References

[1] Y. Tabata, Y. Ito, S. Tagawa (Eds.), CRC Handbook of Radiation Chemistry, CRC Press, Boston, 1991.
[2] S.F. Dainton, M.B. Ledger, R. May, G.A. Salmon, J. Phys. Chem. 77 (1973) 45.
[3] J.H. Baxendale, P. Wardman, Trans. Faraday Soc. 67 (1971) 2997.
[4] J.K. Thomas, K. Johnson, T. Klippert, R. Lowers, J. Chem. Phys. 48 (1968) 1608.
[5] C.D. Jonah, M.C. Sauer Jr., R. Cooper, A.C. Trifunac, Chem. Phys. Lett. 63 (1979) 535.
[6] H.T. Choi, F. Hirayama, S. Lipsky, J. Phys. Chem. 48 (1967) 1608.
[7] R. Cooper, J.K. Thomas, J. Chem. Phys. 48 (1968) 5097.
[8] G.J. Kavarnos (Ed.), Fundamentals of Photoinduced Electron Transfer, Wiley, New York, 1993.
[9] H. Mohan, O. Brede, J.P. Mittal, J. Photochem. Photobiol. A 140 (2001) 191.
[10] S. Samori, M. Hara, S. Tojo, M. Fujitsuka, S.-W. Yang, A. Elangovan, T.-I. Ho, T. Majima, J. Phys. Chem. B 109 (2005) 11735.
[11] S. Samori, S. Tojo, M. Fujitsuka, S.-W. Yang, A. Elangovan, T.-I. Ho, T. Majima, J. Org. Chem. 70 (2005) 6661.
[12] S. Samori, S. Tojo, M. Fujitsuka, S.-W. Yang, T.-I. Ho, J.-S. Yang, T. Majima, J. Phys. Chem. B 110 (2006) 13296.
[13] S. Samori, S. Tojo, M. Fujitsuka, H.-J. Liang, T.-I. Ho, J.-S. Yang, S.-W. Yang, T. Majima, J. Org. Chem. 71 (2006) 8732.
[14] A. Elangovan, T.-Y. Chen, C.-Y. Chen, T.-I. Ho, Chem. Commun. (2003) 2146.
[15] A. Elangovan, S.-W. Yang, J.-H. Lin, K.-M. Kao, T.-I. Ho, Org. Biomol. Chem. 2 (2004) 1597.
[16] A. Elangovan, H.-H. Chiu, S.-W. Yang, T.-I. Ho, Org. Biomol. Chem. 2 (2004) 3113.
[17] A. Elangovan, K.-M. Kao, S.-W. Yang, Y.-L. Chen, T.-I. Ho, Y.O. Su, J. Org. Chem. 70 (2005) 4460.
[18] S.-W. Yang, A. Elangovan, K.-C. Hwang, T.-I. Ho, J. Phys. Chem. B 109 (2005) 16628.
[19] J.-H. Lin, A. Elangovan, T.-I. Ho, J. Org. Chem. 70 (2005) 7397.
[20] S. Samori, S. Tojo, M. Fujitsuka, J.-H. Lin, T.-I. Ho, J.-S. Yang, T. Majima, J. Chin. Chem. Soc. 53 (2006) 1225.
[21] L.R. Faulkner, A.J. Bard, Electroanalytical Chemistry, vol. 10, Marcel Dekker, New York, 1977, pp. 1–95.
[22] A.J. Bard, L.R. Faulkner, Electrochemical Methods Fundamentals and Applications, second edition, John Wiley and Sons, New York, 2001, pp. 736–745.
[23] M.M. Richter, Chem. Rev. 104 (2004) 3003.
[24] A.C. Edwin, W.L. James, E.V. Robert, J. Am. Chem. Soc. 87 (1965) 3259.
[25] M.S. Theodore, B.M. Harry Jr., J. Am. Chem. Soc 94 (1972) 9020.
[26] J.T. Maloy, A.J. Bard, J. Am. Chem. Soc 93 (1971) 5968.
[27] R.Y. Lai, X. Kong, S.A. Jenekhe, A.J. Bard, J. Am. Chem. Soc. 125 (2003) 12631.
[28] A. Kapturkiewicz, Chem. Phys. 166 (1992) 259.
[29] M. Kawai, K. Itaya, S. Toshima, J. Am. Chem. Soc. 84 (1980) 2368.
[30] R.Y. Lai, J.J. Fleming, B.L. Merner, R.J. Vermeij, G.J. Bodwell, A.J. Bard, J. Phys. Chem. A 108 (2004) 376.
[31] J. Strauβ, J. Daub, Adv. Mater. 14 (2002) 1652.
[32] J.C. Scaiano, Handbook of Organic Photochemistry, vol. 1, CRC Press, Boca Raton, FL, 1989, p. 231.
[33] G.A. Reynolds, K.H. Drexhage, Opt. Commun. 13 (1975) 222.
[34] R.R. Hentz, W.V. Sherman, J. Phys. Chem. 73 (1969) 2676.
[35] S.L. Murov, I. Carmichael, G.L. Hug, Handbook of Photochemistry, second edition, Marcel Dekker, New York, 1993.
[36] A. Beeby, K. Findlay, P.J. Low, T.B. Marder, J. Am. Chem. Soc. 124 (2002) 8280.
[37] Y. Croonen, E. Gelade, M. Van der Zegel, M. Van der Auweraer, H. Vandendriessche, F.C. De Schryver, M. Almgren, J. Phys. Chem. 87 (1983) 1426.
[38] Y. Mao, J.K. Thomas, J. Org. Chem. 58 (1993) 6641.
[39] D.K.K. Liu, L.R. Faulkner, J. Am. Chem. Soc. 99 (1977) 4594.
[40] C. Bohne, E.B. Abuin, J.C. Scaiano, J. Am. Chem. Soc. 112 (1990) 4226.
[41] E.M. Gross, J.D. Anderson, A.F. Slaterbeck, S. Thayumanavan, S. Barlow, Y. Zhang, S.R. Marder, H.K. Hall, M.F. Nabor, J.-F. Wang, E.A. Mash, N.R. Armstrong, R.M. Wightman, J. Am. Chem. Soc. 122 (2000) 4972.
[42] J. Mohanty, H. Pal, A.V. Sapre, J. Chem. Phys. 116 (2002) 8006.
[43] T.D. Santa Cruz, D.L. Akins, R.L. Birke, J. Am. Chem. Soc. 98 (1976) 1677.
[44] K. Kilsa, J. Kajanus, A.N. Macpherson, J. Martensson, B. Albinsson, J. Am. Chem. Soc. 123 (2001) 3069.
[45] M.P. Fasnacht, N.V. Blough, Environ. Sci. Technol. 36 (2002) 4364.
[46] P. Cremonesi, E. Rogan, E. Cavalieri, Chem. Res. Toxicol. 5 (1922) 346.
[47] A.M. Swinnen, M. Van der Auweraer, F.C. De Schryver, K. Nakatani, T. Okada, N. Mataga, J. Am. Chem. Soc. 109 (1987) 321.
[48] F.G. Bordwell, J.P. Cheng, M.J. Bausch, J. Am. Chem. Soc. 110 (1988) 2867.
[49] F. Wilkinson, C. Tsiamis, J. Am. Chem. Soc. 105 (1983) 767.
[50] K.M. Maness, J.E. Bartelt, R.M. Wightman, J. Phys. Chem. 98 (1994) 3993.
[51] J. González-Velasco, J. Phys. Chem. 92 (1988) 2202.
[52] K. Itoh, K. Honda, Chem. Lett. 8 (1979) 99.
[53] G.J. Hoytink, Discuss. Faraday Soc. 45 (1968) 14.
[54] I.R. Gould, D. Ege, S.L. Mattes, S. Farid, J. Am. Chem. Soc. 109 (1987) 3794.
[55] H. Tachikawa, A.J. Bard, Chem. Phys. Lett. 2 (1974) 246.